Langmuir

Article

pubs.acs.org/Langmuir

Enhanced Integrin Mediated Signaling and Cell Cycle Progression on Fibronectin Mimetic Peptide Amphiphile Monolayers

Kamlesh Shroff,[†] Timothy R. Pearce,[‡] and Efrosini Kokkoli*,[†]

[†]Department of Chemical Engineering and Materials Science and [‡]Department of Biomedical Engineering, University of Minnesota, Minneapolis, Minnesota 55455, United States

ABSTRACT: In recent years, a variety of biomimetic constructs have emerged which mimic the bioactive sequences found in the natural extracellular matrix (ECM) proteins such as fibronectin (FN) that promote cell adhesion as well as proliferation on artificially functionalized interfaces. Much interest lies in investigating the ability of the ECM mimetic materials in regulating a number of vital cell functions including differentiation, gene expression, migration, and proliferation. A peptide amphiphile PR_b containing both the cell adhesive GRGDSP and synergistic PHSRN peptide sequences was developed in our group that was shown to support enhanced cell proliferation and ECM FN secretion as compared to GRGDSP and FN functionalized interfaces. In this study, we have investigated the binding affinity of the PR_b peptide ligand with the FN cell surface receptor, the $\alpha_5\beta_1$ integrin. We compared PR_b functionalized surfaces with FN and BSA coated surfaces and GRGDSP functionalized surfaces in terms of promoting intracellular signaling cascades that are essential for enhanced cellular activity. Specifically, we studied the phosphorylation of focal adhesion kinase (FAK) at tyrosine residues Y397 and Y576 and the formation of cyclin D1, both of which are intracellular markers of integrin mediated attachment of cells, signaling pathways, and progression of cell cycle. FAK and cyclin D1 encourage enhanced cell proliferation, differentiation, and gene expression. Our results show that the PR_b peptide ligand has a specific and strong binding affinity for the $\alpha_5\beta_1$ integrin with a dissociation constant of 76.3 ± 6.3 nM. The PR_b peptide ligands supported enhanced FAK phosphorylation activity and increased cyclin D1 formation as compared to the widely used GRGDSP ligand, the native protein FN (positive control), and BSA nonadhesive surfaces (negative control). These results encourage the use of the FN mimetic PR_b peptide in functionalizing biomaterials for potential tissue engineering and therapeutic applications.

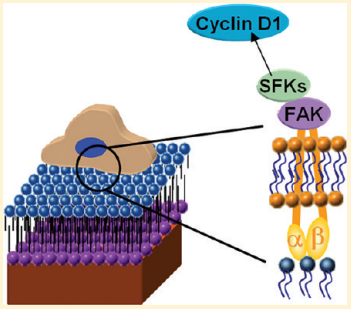

INTRODUCTION

Extracellular matrix (ECM) mimetic biomaterials are rapidly emerging at the forefront of regenerative medicine and tissue engineering. ECM proteins, or synthetic biomimetic peptides that promote specific and desirable biological interactions of the living cells with the material interfaces, are being increasingly used to functionalize materials in biomedical applications. Efforts are focusing in incorporating chemical signals inspired by ECM proteins in order to control cell adhesion, promote cell signaling and cell organization, and ultimately provide an artificial environment which may function as the native tissue or promote its formation.[1−10] The association of cells with the ECM proteins initiates the assembly of specific cell−matrix adhesion sites called focal adhesions that are essential for cell migration as well as activation of adhesion mediated signaling events, thereby regulating cell behavior. Key cell mediators of both matrix attachment and signaling responses are the integrins, which are heterodimeric transmembrane receptors for ECM components.[11,12] Particularly, the $\alpha_5\beta_1$ integrin mediated signaling is central to a variety of cell adhesion related events that control the physiology, migration, proliferation, and differentiation of the cells in vivo as well as in vitro and have been found to dramatically impact a number of phenomena and diseases like wound healing, Alzheimer's disease, and numerous anticancer strategies.[13−20] Integrin binding and focal adhesion assemblies are therefore critical to cellular responses toward biomaterial surfaces in biomedical applications.

A promising strategy to mimic the $\alpha_5\beta_1$−FN interaction is by using short bioactive peptides like the arginine-glycine-aspartic acid (RGD) containing ligands that mimic the integrin binding domain from type III module 10 of FN. RGD is also present in several other ECM proteins and is well-known to promote cell attachment and spreading;[4,7,21,22] however, it has a broad specificity for many adhesion receptors, including $\alpha_5\beta_1$ and $\alpha_v\beta_3$ integrins,[23] which limits its targeted therapeutic use. Apart from glycine-arginine-glycine-aspartic acid-serine-proline (GRGDSP), an additional sequence proline-histidine-serine-arginine-asparagine (PHSRN) present in the FN type III module 9, a synergy site, is needed for high affinity recognition by the $\alpha_5\beta_1$ integrin.[24−26] Our studies suggest that an equimolar mixture of GRGDSP and PHSRN ligands randomly presented at the interface does not offer much advantage over GRGDSP and special design considerations of a peptide containing both ligands is needed.[27] The attachment of endothelial cells to RGD ligands is mediated by both $\alpha_5\beta_1$ and $\alpha_v\beta_3$ integrins, while $\alpha_v\beta_3$ integrins have more of an effect, and attachment to peptides containing both the GRGDSP and PHSRN ligands is

Received: August 23, 2011
Revised: November 29, 2011
Published: December 7, 2011

   dx.doi.org/10.1021/la203322t | *Langmuir* 2012, 28, 1858−1865

attributed to the $\alpha_5\beta_1$ integrins.[27−32] This differential integrin engagement is particularly critical, as more and more evidence now suggests that the specificity of integrin interactions is primarily the key step in cell proliferation and differentiation.[33] The $\alpha_5\beta_1$ integrin and FN therefore form a prototypic integin−ligand pair[23,34,35] that is functionally very important as it mediates fibronectin fibril formation and governs ECM assembly that is vital to cell functions in vivo.[36] A number of biomimetic FN designs appeared in the literature that contain both the GRGDSP and PHSRN ligands, but their success is limited.[37−41] We have designed the PR_b peptide that mimics both the distance and hydrophobicity/hydrophilicity between RGD and PHSRN in FN.[27,29,31,42] The PR_b peptide amphiphile contains a hydrophobic tail (C_{16} dialkyl ester tail with a glutamic acid (Glu) tail connection and a $(CH_2)_2$ tail spacer, $(C_{16})_2$-Glu-C_2-) connected to the PR_b peptide headgroup that has four building blocks, a lysine-serine-serine (KSS) spacer, PHSRN, a $(SG)_5$ linker, and RGDSP.[27] PR_b functionalized surfaces have been shown to not only support enhanced cell adhesion and proliferation over its counterpart GRGDSP that is widely used but also have surpassed FN surfaces in terms of promoting cell adhesion, proliferation, and ECM production and thus have been used in tissue engineering and drug delivery applications.[27,43−49] The PR_b peptide sequence has been previously reported to bind specifically to the $\alpha_5\beta_1$ integrin.[27] Recently it has been shown that polymersomes functionalized with the PR_b peptide do not bind to $\alpha_5\beta_1$-expressing CT26 colon cancer cells that have been preincubated with the anti-$\alpha_5\beta_1$ antibody or, in the absence of any blocking antibodies, to Caco-2 cells that express the $\alpha_v\beta_3$ integrin and show only minimal expression of $\alpha_5\beta_1$ integrin.[50]

ECM proteins and biomimetic peptides such as PR_b engage integrin receptors on the cell surface and recruit a number of intracellular proteins to specialized sites of the cytoplasm into focal adhesions. These focal adhesion plaques are composed of several proteins that include kinases, phosphatases, scaffolding proteins, and G-proteins.[51] The assembly of protein complexes also functions to anchor actin filament bundles, thereby providing the physical support necessary for cell spreading, locomotion, and growth.[52] Integrin binding, activation, and clustering leads to the tyrosine phosphorylation of cytoplasmic proteins, such as focal adhesion kinase (FAK), Src, paxillin (Pax), tensin, and p130Cas. FAK and Src are among the first few protein tyrosine kinases to get recruited at the sites of integrin engagement and act as the key members of the focal adhesion complex.[15,16,51] FAK is phosphorylated during cell adhesion to FN[53] and is thought to lead the activation of many diverging signaling pathways[54] critical for cell adhesion dependent growth and survival, proliferation, gene expression,[55] and migration.[56] Figure 1 shows a schematic of some of the important steps and molecules involved in the integrin signaling pathways. FAK associates with the transmembrane integrins, and this results in its autophosphorylation (process in which a kinase attaches a phosphate group to itself) at the tyrosine residue 397 (Y397). This autophosphorylation occurs immediately after integrin clustering and creates high affinity binding sites for the SH_2 domains of several important signaling proteins, thus allowing the FAK to associate with Src (for subsequent FAK phosphorylations), PI-3K (plays a role in conjunction with FAK in cell proliferation and migration), p130Cas (important for cell migration), and Pax (localize with FAK and plays a role in cell spreading).[57] In addition to Y397, five other tyrosine residues are phosphorylated (407, 576, 577, 861, and 925). Y576 and Y577 that are contained in the kinase domain of the FAK are phosphorylated via the Src binding and are critically required for maximal catalytic activity of the FAK immune complexes that are formed upon cell adhesion.[58,52] Hence, the autophosphorylation of FAK at Y397 (FAK [pY397]) creates a binding site for Src family kinases that in turn serves to phorphorylate additional tyrosine residues of FAK (e.g., Y576), and this positive loop of both trans- and cis-phosphorylation increases the overall FAK kinase activity and the FAK-dependent downstream signaling.[58−61] We therefore decided to study the expression of FAK, considering it as one of the early events of integrin mediated signaling, and its phosphorylation at two important tyrosine residues, namely Y397 and Y576 (FAK [pY397] and FAK [pY576]).

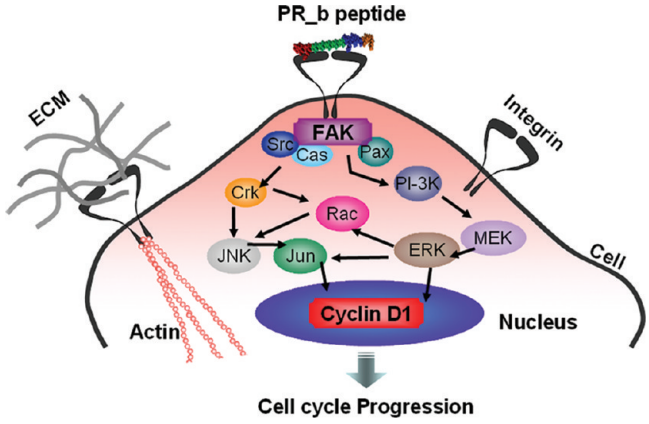

Figure 1. Schematic of major integrin linked signaling pathways that start with phosphorylation of focal adhesion kinase (FAK) upon cell attachment. FAK phosphorylation in turn allows the FAK to associate with Src and activate Cas and Pax that lead to the activation of a number of other molecules downstream and prepare the cell for proliferation by upregulating cyclin D1.

A number of recent studies have demonstrated an effective link between ECM FN and integrin mediated cell adhesion to the regulation of cell cycle progression.[62−65] For example, integrins have been reported to activate molecules further downstream in signaling pathways, such as Rac which controls progression through the G1 phase of the cell cycle.[66] Figure 1 highlights a few key intracellular signals that link FAK to a variety of signaling molecules which interconnect and affect cell cycle progression. For example, the FAK−Src complex formed after the phosphorylation of FAK Y397 (FAK [pY397]) promotes phosphorylation of FAK Y576 (FAK [pY576]) and Pax and also the activation of other signaling molecules such as Cas. These in turn lead to localization of Crk in focal adhesion and also the activation of signaling molecules such as JNK and Rac that play an important role in cell cycle progression.[10,15] Evidence points out that the FAK−Src complex formed as a result of FAK [pY397] may also transmit downstream signals in the form of activation of the other important pathways that influence cell proliferation, cell cycle progression, and survival through the activity of PI-3K and cyclins.[65,67−71]

Integrin mediated cell adhesion controls cell cycle proliferation by regulating the expression and activities of cyclins. In general, the key cyclins involved in the cell cycle progression from G1-to-S phase are cyclins D, E, and A. Cyclin D1 is believed to function as a key regulator of cell cycle progression and was recently indicated as a functional target of integrin mediated FAK signaling pathways.[65,72−74] For example, integrin

dx.doi.org/10.1021/la203322t | Langmuir 2012, 28, 1858−1865

mediated FAK signaling was found to promote transcriptional activation of the cyclin D1 gene via ERK pathway, and as a result increased cyclin D1 mRNA accumulation was observed in NIH3T3 fibroblasts cells.[73] In addition, several studies have shown that the expression levels of cyclin D1 are rate limiting in cellular proliferation.[75−77] Cyclin D1 expression has been found to be anchorage dependent and is decreased upon changes in cell shape and cytoskeletal tension.[77] These findings highlight the importance of cyclin D1 and its expression levels on the proliferation of cells attaching to various types of adhesive ligands.

In this study we investigate the binding affinity of PR_b for the $\alpha_5\beta_1$ integrin and examine whether the PR_b binding influences the integrin mediated signaling that is known to highly affect the activity of cells, like migration, differentiation, or proliferation. In particular, we examine whether the anchorage of cells to different surfaces promotes expression of FAK and its phosphorylation at tyrosine residues Y397 and Y576. As a step further, we quantitatively compare the formation of the cell cycle progression marker cyclin D1. The distribution of the above marker proteins is directly visualized inside the cells by performing immunofluorescence staining of both the phosphorylated FAK tyrosine residues and cyclin D1. The surfaces examined are the PR_b and GRGDSP peptide surfaces, FN (positive control), and bovine serum albumin (BSA) which is known to prevent adhesion (negative control).

MATERIALS AND METHODS

All chemicals were purchased from Sigma-Aldrich except otherwise stated. Water that was purified to a resistivity of 18.2 MΩ cm^{-1} was obtained from a Milli-Q water system (Millipore) and sterilized by autoclaving prior to use.

Synthesis of Peptides and Peptide Amphiphiles. The PR_b peptide sequence (KSSPHSRN(SG)$_5$RGDSP), biotinylated PR_b peptide (Biotin-KSSPHSRN(SG)$_5$RGDSP), scrambled biotinylated PR_b peptide (Biotin-SGRSGSGSHGGDSGSSKSSNPPR), and the GRGDSP peptide sequences were synthesized by the Oligonucleotide and Peptide Synthesis Facility at the University of Minnesota. The PR_b peptide amphiphile, $(C_{16})_2$-Glu-C_2-KSSPHSRN(SG)$_5$RGDSP, and GRGDSP peptide amphiphile, $(C_{16})_2$-Glu-C_2-GRGDSP, used in this study were synthesized as described in the literature.[78]

Saturation Binding Experiments of PR_b. A modified ELISA method was performed to assess the binding affinity of the PR_b ligand for the $\alpha_5\beta_1$ integrin receptor. 50 ng of recombinant human integrin $\alpha_5\beta_1$ (R&D Systems, catalog number 3230-A5-050) suspended in phosphate buffer saline (PBS) supplemented with 1 mM $MnCl_2$ (PBS/Mn^{2+}) was added to 96-well plates (Thermo Scientific, catalog number 439454) overnight at 4 °C. Excess $\alpha_5\beta_1$ was removed, and wells were washed once with washing buffer (PBS/Mn^{2+} and 0.05% Tween-20). 200 μL of washing buffer was added to the wells, and the plates were gently agitated by hand for 10 s, followed by decanting the liquids from the wells by inverting the plate and tapping on paper towels 2−3 times. This procedure was repeated twice for a single washing step. All wells were blocked for 2 h at room temperature with 2% BSA (Thermo Scientific, catalog number SH30574.02) in PBS/Mn^{2+} buffer. Biotinylated PR_b peptide solutions with concentrations ranging from 0 to 60 μM were created from a 600 μM stock solution by dilution with PBS/Mn^{2+} buffer containing 0.1% BSA and added to wells in triplicate. After the plates were incubated at room temperature (so that our results could be compared with K_D values for FN)[26,79,80] for 2 h on an orbital shaker, the PR_b solutions were removed, and wells were washed three times with washing buffer. A 50 μL neutravidin−horseradish peroxidase (Thermo Scientific, catalog number 31030) solution at concentration of 1 μg/mL in PBS/Mn^{2+} buffer with 1% BSA was added, and plates were incubated for 30 min at room temperature. After five washes with the washing buffer, 3,3′,5,5′-tetramethylbenzidine (TMB) (Promega Corp., Madison, WI, catalog W4121) substrate was added to all wells and allowed to oxidize for 20 min before a 1 M H_2SO_4 stop solution was added and absorbance at 450 nm recorded from each well. To measure the background binding, the biotinylated PR_b solutions were added to wells without integrin $\alpha_5\beta_1$ and developed in an identical manner. Binding data from individual experiments were averaged, followed by analysis using a nonlinear least-squares regression analysis fit to $B = B_{max} \times [PR\_b]/(K_D + [PR\_b])$ to determine K_D and B_{max}, where B is binding, B_{max} is saturated binding, [PR_b] is the PR_b concentration, and K_D is the dissociation constant.[81,82]

Preparation of Surfaces. The Langmuir−Blodgett (LB) technique was used to create supported peptide amphiphile bilayer membranes as described elsewhere.[29] Briefly, 87 nmol of 1,2-distearoyl-*sn*-glycero-3-phosphoethanolamine (DSPE, Avanti Polar Lipids, Inc., catalog number 110634) was initially spread at the air−water interface of the LB trough, compressed to a surface pressure of 45 mN/m, and stabilized for 10 min. The compressed DSPE monolayer was transferred to the 22 mm circular mica substrates by pulling them vertically out of the water, thereby depositing the hydrophilic headgroups on the mica surface and the carbon tails exposed to air. Immediately after that a monolayer of PR_b (32 nmol) or GRGDSP (93 nmol) was spread at a clean air−water interface, compressed to 45 mN/m, and allowed to stabilize for 10 min. Peptide amphiphile monolayers were transferred to the DSPE coated mica substrates by the vertical dipping method into the water subphase. At the time of transfer, the average mean molecular areas and transfer ratios from several depositions were 42 ± 4 $Å^2$ and 0.95 ± 0.07 for DSPE, 65 ± 4 $Å^2$ and 0.85 ± 0.14 for PR_b, and 41 ± 7 $Å^2$ and 0.98 ± 0.10 for GRGDSP. The LB peptide amphiphile films were always kept under water without exposing to the air, as they are known to rearrange to form multilayers,[83] and they were transferred into 12-well plates (precoated with BSA) containing sterile serum free vascular cell basal media and equilibrated at 37 °C, 5% CO_2, for 30 min before adding the cells. Human fibronectin coated coverslips (FN), 22 mm in diameter (BD Biosciences, catalog number 354088), were similarly equilibrated at 37 °C, 5% CO_2, for 30 min in the same serum-free media.

Cell Culture. Primary human umbilical vein endothelial cells (HUVEC, catalog number PCS-100-010), vascular cell basal media (catalog number PCS-100-030), and the endothelial cell growth kit (catalog number PCS-100-041) were purchased from American Type Culture Collection (ATCC). The HUVECs were cultured in the vascular cell basal medium supplemented with VEGF endothelial cell growth kit according to ATCC's instructions. The culture flasks were incubated at 37 °C and 5% CO_2, and the media were changed every alternate day until confluency was reached. The cells used in this study were in passages 3 and 4 as previous work in our lab has shown that higher passages did not give reproducible cell proliferation results.

Western Blot Analysis. This analysis was performed as discussed in the literature.[84−86] Briefly, cells were trypsinized from the culture plates, resuspended and gently agitated for 45 min in serum-free media, and seeded on each surface at 500 cells/mm^2 in serum-free media for 2 h. Cells were lysed in RIPA buffer (10 mM tris-hydrochloride pH 7.4, 100 mM sodium chloride, 1 mM ethylenediaminetetraacetic acid, 1 mM ethylene glycol tetraacetic acid, 1 mM sodium fluoride, 2 mM sodium orthovanadate, 0.1% sodium dodecyl sulfate, 0.5% sodium deoxycholate, 1% Triton X-100, 1 mM phenylmethanesulfonyl fluoride, 60 μg/mL aprotinin (Roche Applied Science, catalog number 10236624001), 10 μg/mL leupeptin (Roche Applied Science, catalog number 11017101001), 1 μg/mL pepstatin) for 20 min on ice while repeatedly pipetting up and down for several times. Cellular debris was removed by centrifuging the lysates at 14000*g* for 10 min. The clarified lysates were decanted into sterile clean tubes and concentrated using Microcon YM10 (10 kDa MW cutoff, Millipore, catalog number 42406) centrifugal filters, and the total protein was quantified using a micro-BCA (bicinchoninic acid) protein assay reagent kit (Pierce Scientific, Rockford, IL; catalog number 23235). 20 μg of protein used per lane was boiled at 100 °C for 90 s in Laemmli buffer (65 mM Tris, pH 6.8, 5% glycerol, 5% SDS,

dx.doi.org/10.1021/la203322t | *Langmuir* 2012, 28, 1858−1865

0.003% bromophenol blue, and 65 mM dithiothreitol) and electrophoretically resolved on a 7.5% polyacrylamide gel (Tris-HCl readygel, Bio-Rad, catalog number 161-1100). Protein bands (125 kDa for FAK and 36 kDa for cyclin D1) were identified by their migration on the gel and compared to a commercially available molecular weight (MW) marker (protein ladder, Bio-Rad, catalog number 161-0373) that was run into a separate lane. The proteins were then transferred onto a Hybond-P poly(vinylidene fluoride) (PVDF) membrane (GE Healthcare, catalog number RPN303F) using the Western blotting method. The membranes were blocked with 5% immunoglobulin free BSA (Sigma-Aldrich, catalog number A3059) in Tris buffered saline (TBS) with 0.1% Tween-20 and incubated separately with primary antibodies (Invitrogen) to FAK (catalog number AHO0502), FAK [pY397] (catalog number 44624G), FAK [pY576] (catalog number 44652G), and cyclin D1 (catalog number AHF0102) for 2 h. After washing, the membranes were incubated with an enzyme conjugated secondary antibody, goat anti-rabbit IgG alkaline phosphatase and further developed using the enhanced chemifluorescent (ECF) substrate according to the instructions from the ECF Western blotting kit (GE Healthcare, catalog number RPN5783). The fluorescent bands were scanned on a Molecular Dymamics Storm-840 flatbed densitometer using a 570 nm filter in the fluorescence mode and quantified using the NIH Image-J software.

Immunofluorescence Staining. Cells were cultured and seeded as described above on PR_b, FN, GRGDSP, and BSA coated substrates. At the end of the 2 h incubation, cells were fixed in 4% paraformaldehyde solution for 15 min and permeabilized using 0.1% Triton X-100, at 37 °C and 5% CO_2. All the above four surfaces were separately incubated at 37 °C and 5% CO_2 first with anti-FAK [pY-397], anti-FAK [pY-576], and anticyclin D1 primary antibodies (Invitrogen) for 2 h, followed by incubation with a fluorescein isothiocynate (FITC) conjugated anti-rabbit secondary antibody (Millipore, catalog number 656111) for 1 h at similar conditions. As a final step, the actin filaments were fluorescently stained with tetramethylrhodamine isothiocynate (TRITC) conjugated phalloidin, and nuclei were stained using the 4′,6-diamidino-2-phenylindole (DAPI) from the Actin Cytoskeleton/Focal adhesion staining kit (Millipore, catalog number FAK100) according to manufacturer's instructions. The surfaces were carefully removed from the 12-well plates and mounted onto glass slides in ProLong Gold antifade reagent (Invitrogen, catalog number P36934) and stored at 4 °C protected from light. An Olympus FluoView 1000 IX2 inverted confocal microscope at the Biomedical Image Processing Lab at the University of Minnesota was used for imaging.

RESULTS AND DISCUSSION

In this study we first investigated the binding affinity and specificity of the PR_b ligand to the $\alpha_5\beta_1$ integrin receptor. Binding affinities are often represented by the equilibrium dissociation constants that offer an assessment of the strength of the binding of a ligand to the receptor. To evaluate the binding affinity of the PR_b ligand for the $\alpha_5\beta_1$ receptor, a series of saturation binding experiments were performed and analyzed. Identical experiments using a scrambled version of PR_b were also performed to investigate the specificity of the PR_b–$\alpha_5\beta_1$ interaction. The binding of the PR_b and the scrambled PR_b to the $\alpha_5\beta_1$ integrins is plotted in Figure 2. A dissociation constant, K_D, of 76.3 ± 6.3 nM was calculated for the PR_b peptide. It can be also seen from Figure 2 that the binding of the scrambled PR_b was negligible at all the concentrations tested, suggesting a sequence specific interaction between PR_b and integrin $\alpha_5\beta_1$. The affinity of the PR_b peptide for $\alpha_5\beta_1$ (76.3 ± 6.3 nM) is strikingly stronger than that of the GRGDdSP peptide (270 ± 353 μM),[87] which lacks the PHSRN synergy site found on PR_b, and is only moderately weaker than the FN–$\alpha_5\beta_1$ interaction reported as 30 nM (FN using ELISA),[79] 4.4 nM (FN 7–10 fragment

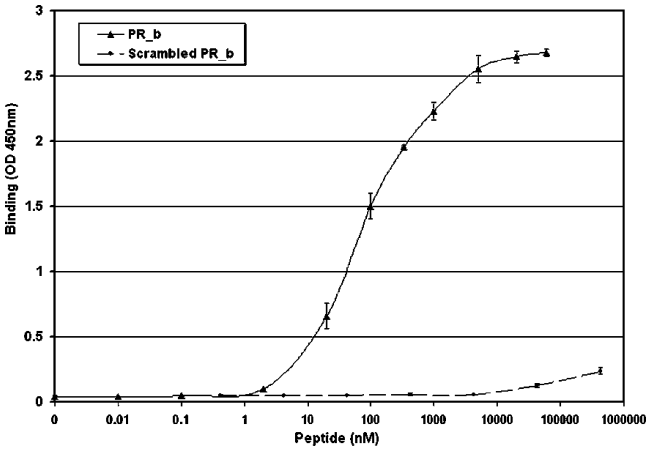

Figure 2. Saturation binding curves of PR_b and scrambled PR_b to the $\alpha_5\beta_1$ integrins determined using a modified ELISA method. The K_D of PR_b was evaluated to be 76.3 ± 6.3 nM. The values represent the mean ± SD of three separate experiments for PR_b (n = 3) and two separate experiments for scrambled PR_b (n = 2). All experiments were performed in triplicate. The minimal signal (close to baseline) for the scrambled version of PR_b demonstrates the specific nature of the PR_b–integrin $\alpha_5\beta_1$ interaction.

quantified with surface plasmon resonance),[80] 2 nM (FN 9–10 fragment using ELISA),[26] and 17 nM (FN 9–10 fragment using surface plasmon resonance).[26] This improvement in the affinity of the PR_b peptide over the commonly used GRGDdSP peptide combined with PR_b's specific binding to the $\alpha5\beta1$ integrin demonstrates the potential of this FN mimetic peptide.

The ability of PR_b to potentially influence the intracellular pathways compared to FN and GRGDSP surfaces was investigated next. For that we examined whether GRGDSP, PR_b, FN, and BSA surfaces could modulate HUVEC intracellular signaling by analyzing the expression of FAK, FAK [pY397], and FAK [pY576] following a 2 h cell adhesion on each of the above surfaces in serum-free media. Figure 3A shows representative Western blot strips corresponding to FAK [pY397], FAK [pY576], and FAK expression, and Figure 3B gives a quantification of the Western blot results for FAK [pY397] and FAK [pY576] divided by the total FAK and normalized to that of FN surfaces for easy comparison. It can be seen from Figure 3A that the phoshorylated FAK at its tyrosine residues Y397 and Y576 expressed by the cells on BSA coated substrates is close to basal level. The quantification of the bands reveals a clear trend in the phosphorylation activity at each surface as presented in Figure 3B. The FAK [pY397]/FAK is 1.3 times higher on PR_b, 0.52 times on GRGDSP, and 0.31 times on the BSA surfaces as compared to the FN surfaces. Likewise, the FAK [pY576]/FAK follows a similar trend as in the FAK [pY397]/FAK case, with PR_b giving 1.57 times, GRGDSP 0.72 times, and BSA 0.26 times the amount of FAK that is phosphorylated at Y576 to that on FN surfaces. The trends for the phosphorylation activities of FAK at Y397 and Y576 were therefore similar; i.e., phosphorylation is hardly detected on BSA coated substrates (negative control), while the GRGDSP showed lower levels than FN (positive control) and the PR_b appears to promote relatively higher amounts of FAK [pY397] and FAK [pY576] on FAK than FN.

Confocal microscopy was performed on immunofluorescently stained cells for the presence of phosphorylated FAK at Y397 and Y576. Actin stress fibers and nuclei were also labeled.

dx.doi.org/10.1021/la203322t | Langmuir 2012, 28, 1858–1865

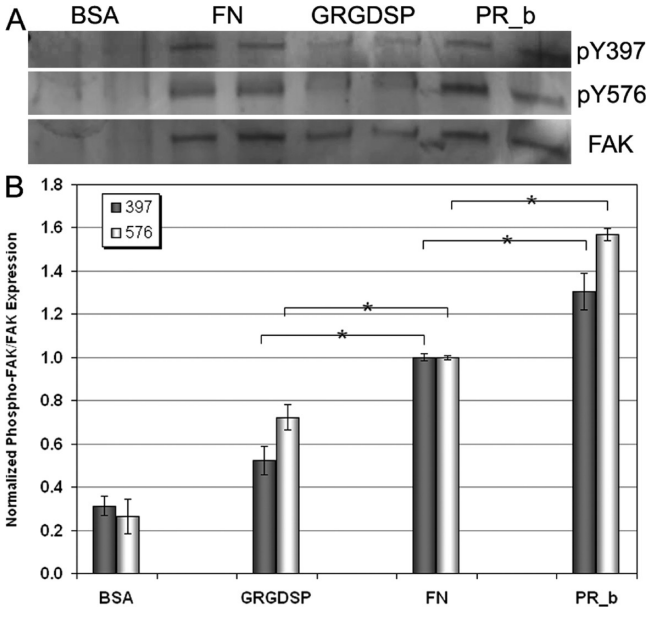

Figure 3. Phosphorylation of site-specific tyrosine residues (pY397 and pY576) of focal adhesion kinase (FAK) in HUVECs seeded for 2 h on PR_b, GRGDSP, FN, and BSA coated surfaces in serum-free media. (A) Representative blots are shown corresponding to pY397, pY576, and FAK. (B) Quantification of Western blot results. The graph shows the relative values of the phosphorylation to total FAK normalized to that of FN surfaces. The values represent the mean ± standard deviation of two separate experiments (n = 2). All experiments were performed in duplicate. Comparison by Z test; *p < 0.001.

Representative confocal images showing FAK [pY397] and FAK [pY576] on different surfaces are presented in Figure 4. BSA coated surfaces (Figure 4A) due to their inert nature support very low actin formation with lack of fibers, and absence of a strong green signal indicating that phosphorylation of Y397 or Y576 was low. The GRGDSP surface (Figure 4B) showed some actin organization and FAK [pY397] and FAK [pY576] activity indicated by the diffused green signal inside the cells. The cells on the GRGDSP surface were not well spread with some cells rather assuming spindle-shaped morhophology, thereby indicating a poor interaction with the surfaces. These results closely resemble previous data that showed poor actin organization on GRGDSP.[27] On the other hand, FN and PR_b surfaces (Figures 4C and 4D, respectively) promoted intense actin formation with distinct fibers that run throughout the cells, quite in agreement with previously published results on both of these surfaces.[27] The presence of green signal on Figures 4C and Figure 4D clearly indicates substantial FAK [pY397] and FAK [pY576] on FN and PR_b surfaces, respectively. On the FN surfaces, for both FAK [pY397] and FAK [pY576], the majority of the green signal was detected in the cytosolic region with some colocalization with focal adhesion points, whereas on the PR_b surfaces the green signal is mostly located at the focal adhesion points, at the ends of actin fibers that are associated with focal adhesion sites. It can be clearly seen that higher amounts of FAK [pY397] and FAK [pY576] are observed on the PR_b surfaces as compared to all the other surfaces, including FN. The results of Figure 4 as can be seen are in agreement with Figure 3, both showing that the PR_b surfaces promote higher phosphorylation activity compared to the other surfaces.

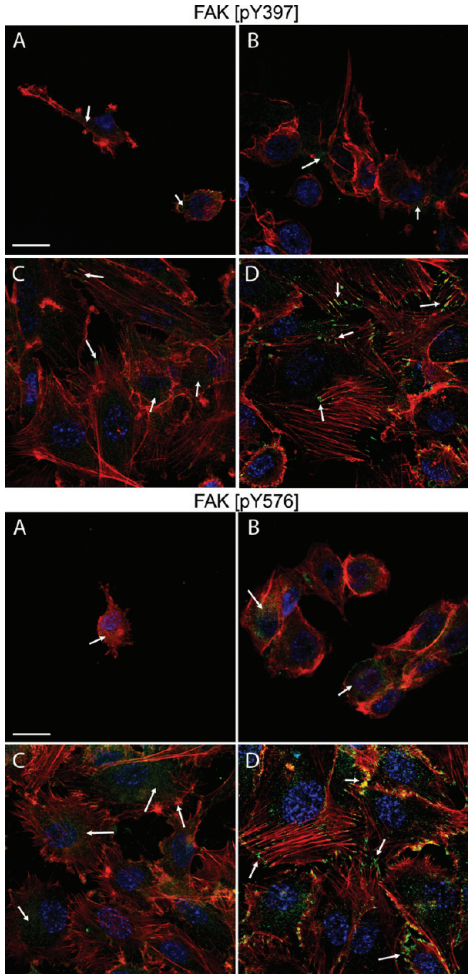

Figure 4. Confocal images of HUVECs stained for FAK [pY397] and FAK [pY576] when seeded on (A) BSA, (B) GRGDSP, (C) FN, and (D) PR_b coated surfaces for 2 h in serum-free media. The scale bar is 20 μm for all images. Phosphorylation of FAK at Y397 and Y576 is indicated by green, actin stress fibers by red, and the nuclei in blue. White arrows show representative expression of FAK [pY397] and FAK [pY576].

Higher phosphorylation on the PR_b surfaces as compared to the FN and GRGDSP surfaces clearly demonstrates that the PR_b cell adhesion ligands can promote and influence the signaling cascades that follow after binding to the integrin receptors. The results of the binding experiments presented in Figure 2 have shown that the PR_b is a promising FN mimetic peptide as evident by its low K_D. We have previously observed higher cell adhesion and proliferation as well as production of ECM on PR_b than on FN and other FN mimetic peptide surfaces, which we attributed to the PR_b sequence accurately mimicking the cell binding domain of FN, and the higher number of PR_b molecules per surface area as compared to the number of FN molecules.[27] However, the latter alone is not a sufficient condition to support higher adhesion on the peptide surfaces since the GRGDSP surfaces also have a higher peptide:FN ratio but promote much less cell adhesion and proliferation than FN.[27] On the basis of the mean molecular areas of the PR_b (65 ± 4 Å^2) and GRGDSP (41 ± 7 Å^2) molecules at the time of deposition, we have theoretically calculated their coating concentrations to be 255 pmol/cm^2 for PR_b and 405 pmol/cm^2 for GRGDSP. The coating concentration of FN was 15−35 μg/mL and corresponded to

dx.doi.org/10.1021/la203322t | Langmuir 2012, 28, 1858−1865

a full monolayer of the protein (information provided by the manufacturer). Experimental studies show that within this range of coating concentrations the fibronectin surface density is 350−450 ng/cm^2.[88] So 400 ng/cm^2 or 0.909 pmol/cm^2 (MW FN 440 kDa; BD Biosciences) represents the amount of fibronectin necessary to produce a monolayer coating. Therefore, at saturation conditions, the ratio of PR_b:FN molecules is 280:1 and for GRGDSP:FN is 445:1. Thus, the combination of a higher number of peptide ligands and the actual sequence of PR_b are both needed to stimulate higher FAK phosphorylation compared to the GRGDSP or FN surfaces.

Previous work in the literature demonstrated that RGD functionalized substrates supported $\alpha_5\beta_1$ mediated cell attachment and FAK signaling; however, it did not surpass the results obtained for the FN control surfaces. For example, in one study it was reported that RGD-based artificial extracellular matrix proteins at a concentration of 4 mg/mL promoted FAK [pY397] on the $\alpha_5\beta_1$ expressing Chinese hamster ovary (CHO) cells; however, it was lower than the phosphorylation activity seen on FN surfaces at 10 μg/mL.[89] It was also found in another study that MC3T3-E1 murine osteoblast-like cells adhered to surfaces with recombinant FN fragments containing both RGD and PHSRN from the 7−10 type III repeats of FN at 150 fmol/cm^2 and promoted higher FAK [pY397] and FAK [p576] as compared to surfaces presenting only RGD at 3000 fmol/cm^2.[84] On the other hand, fibronectin adsorption on surfaces may be challenging, and its presentation and conformation on the interface affect $\alpha_5\beta_1$-mediated signaling events. For example, one study evaluated adhesion of human fibrosarcoma HT1080 cells to saturated levels of FN coatings on untreated polystyrene substrates and found poor to negligible phosphorylation, supporting the fact that changes in FN conformation may adversely affect its signaling capability.[90] Furthermore, simulations studies suggest that the 10th type III repeat of FN is sensitive to unraveling under the application of force (that is in the same range as might be applied by a single fibronectin−integrin bond)[91] and can affect the position and orientation of the RGD loop.[92] That alone may affect integrin binding and subsequent signaling, since studies show that signaling via FAK is proportional to the number of integrin−fibronectin bonds.[93] Therefore, these results suggest that the presentation of peptide ligands can offer a robust approach to functionalizing interfaces other than the conventional FN coatings. Therefore, enhanced phosphorylation activity on PR_b surfaces compared to GRGDSP or FN surfaces may be attributed to the PR_b sequence mimicking more accurately the FN cell adhesion domain than GRGDSP alone and also to the increased number of active ligands that are less prone to denaturation and may be able to form more effective focal contacts,[30] normally associated with high levels of tyrosine phosphorylation.[59]

Integrin mediated FAK phosphorylation and subsequent binding to Src stimulate further downstream signals for cell proliferation. Cyclin D1 is particularly influenced by the Src mediated ERK pathway (Figure 1), and this led us to hypothesize that PR_b or other integrin binding ligands may influence its expression. We therefore investigated the expression of cyclin D1 using Western blot experiments, and the results are presented in Figure 5. The cells on BSA coatings show negligible levels of cyclin D1 as expected from their nonspecific attachment at the interface that does not involve integrins. GRGDSP surfaces perform poorly, and the cyclin D1

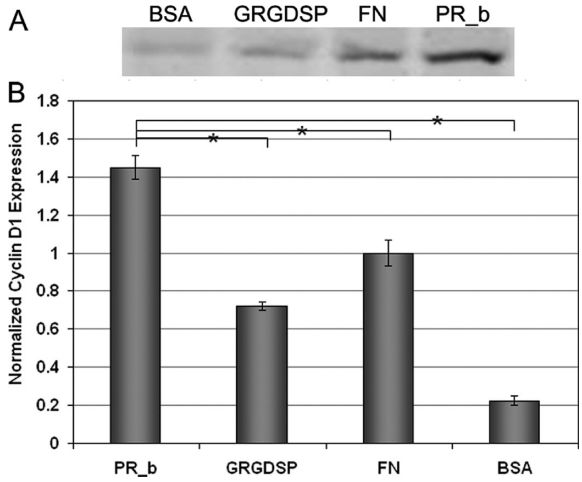

Figure 5. Western blot analysis of cyclin D1 protein on HUVEC lysates. HUVECs were seeded for 2 h on PR_b, GRGDSP, FN, and BSA coated surfaces in serum-free media. (A) Representative bands corresponding to cyclin D1, which showed increased expression on PR_b substrates. (B) Quantification of Western blot results normalized to that of FN surfaces. The values represent the mean ± standard deviation of three separate experiments (n = 3). All experiments were performed in duplicate. Comparison by Z test; *p < 0.001.

formation on PR_b surfaces is 1.45 times higher than FN surfaces. The observed differences in the expression levels of cyclin D1 are in agreement with the trends observed from cell proliferation and spreading experiments performed on HUVECs attaching to the same adhesive ligands from 1 to 72 h (FN surfaces and pure PR_b and GRGDSP LB layers deposited at similar deposition pressures).[27] For example, after 1 h HUVECs proliferated more on PR_b surfaces (256 ± 11 cells/mm^2), followed by FN (210 ± 4 cells/mm^2) and GRGDSP (101 ± 4 cells/mm^2). The higher expression of cyclin D1, which is a cell cycle progression marker, on the PR_b surfaces strengthens our hypothesis that PR_b can effectively modulate integrin mediated signaling from initial to downstream events associated with the cell cycle progression and regulation of cell proliferation. Hence, PR_b appears to have a deeper role than simply participating in the activation and phosphorylation of FAK. Immunofluorescence staining of cyclin D1 is presented in Figure 6 and clearly supports the results obtained from the Western blots in Figure 5. Cyclin D1 can be clearly seen in the nuclear region of the cells, expressed at much higher amounts on HUVECs seeded on the PR_b and FN surfaces compared to the GRGDSP and BSA surfaces. PR_b, therefore, was found to be the most promising ligand compared to the other ligands used in this study and was shown to promote higher phosphorylation of FAK and expression of cyclin D1 that are associated with the integrin mediated signaling pathway.

■ CONCLUSION

PR_b is found to have high affinity (K_D = 76.3 ± 6.3 nM) for the $\alpha_5\beta_1$ integrin while the scrambled sequence showed no binding, thereby showing high specificity of the PR_b sequence for $\alpha_5\beta_1$. PR_b's K_D is a dramatic improvement over the commonly used GRGDdSP peptide (K_D = 270 ± 353 μM) and is 2.5−30 times higher than FN's K_D (K_D values vary between 2 and 30 nM), thereby approaching the affinity of the native

dx.doi.org/10.1021/la203322t | Langmuir 2012, 28, 1858−1865

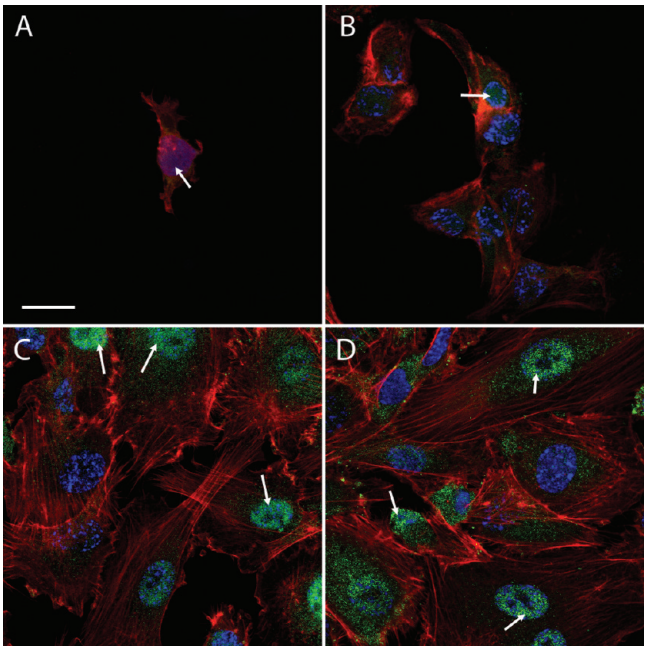

Figure 6. Confocal images of HUVECs showing expression of cyclin D1 when seeded on (A) BSA, (B) GRGDSP, (C) FN, and (D) PR_b coated surfaces for 2 h in serum-free media. The scale bar is 20 μm for all images. Cyclin D1 is shown in green, actin stress fibers in red, and the nuclei in blue. White arrows show representative expression of cyclin D1.

FN–$\alpha_5\beta_1$ integrin interaction. Using the FN mimetic cell adhesive ligand PR_b to functionalize biomaterial interfaces offers a robust approach that promotes higher cell signaling events associated with the binding of the integrin receptor at the cell surface. Activation of signaling pathways that originate at the sites of focal adhesions was dependent on the type of ligand used. PR_b functionalized surfaces supported higher FAK phosphorylation at Y397 and Y576 and cyclin D1 expression compared to other supports, such as GRGDSP, FN, and BSA surfaces, as evident by Western blots and confocal images. Our findings suggest that PR_b is a promising FN mimetic peptide.

AUTHOR INFORMATION

Corresponding Author

*E-mail kokkoli@umn.edu; Tel 612-626-1185; Fax 612-626-7246.

ACKNOWLEDGMENTS

This work was supported in part by the Camille Dreyfus Teacher-Scholar Awards Program and by the MRSEC Program of the National Science Foundation under Award DMR-0819885.

REFERENCES

(1) Lutolf, M. P.; Hubbell, J. A. *Nature Biotechnol.* **2005**, *23* (1), 47–55.
(2) Webber, M. J.; Tongers, J.; Renault, M. A.; Roncalli, J. G.; Losordo, D. W.; Stupp, S. I. *Acta Biomater.* **2010**, *6* (1), 3–11.
(3) Ma, P. X. *Adv. Drug Delivery Rev.* **2008**, *60* (2), 184–198.
(4) Perlin, L.; MacNeil, S.; Rimmer, S. *Soft Matter* **2008**, *4* (12), 2331–2349.
(5) Storrie, H.; Guler, M. O.; Abu-Amara, S. N.; Volberg, T.; Rao, M.; Geiger, B.; Stupp, S. I. *Biomaterials* **2007**, *28* (31), 4608–4618.
(6) Garcia, A. J. *Polym. Regener. Med.* **2006**, 171–190.
(7) Hersel, U.; Dahmen, C.; Kessler, H. *Biomaterials* **2003**, *24* (24), 4385–4415.
(8) von der Mark, K.; Park, J.; Bauer, S.; Schmuki, P. *Cell Tissue Res.* **2010**, *339* (1), 131–153.
(9) Daley, W. P.; Peters, S. B.; Larsen, M. *J. Cell Sci.* **2008**, *121* (3), 255–264.
(10) Wozniak, M. A.; Modzelewska, K.; Kwong, L.; Keely, P. J. *Biochim. Biophys. Acta, Mol. Cell Res.* **2004**, *1692* (2–3), 103–119.
(11) Hynes, R. O. *Cell* **1992**, *69* (1), 11–25.
(12) Clark, E. A.; Brugge, J. S. *Science* **1995**, *268* (5208), 233–239.
(13) Giancotti, F. G.; Ruoslahti, E. *Science* **1999**, *285* (5430), 1028–1032.
(14) Boudreau, J.; Jones, P. L. *Biochem. J.* **1999**, *339*, 481–488.
(15) Romer, L. H.; Birukov, K. G.; Garcia, J. G. N. *Circ. Res.* **2006**, *98* (5), 606–616.
(16) Hehlgans, S.; Haase, M.; Cordes, N. *Biochim. Biophys. Acta, Rev. Cancer* **2007**, *1775* (1), 163–180.
(17) Kim, S.; Bell, K.; Mousa, S. A.; Varner, J. A. *Am. J. Pathol.* **2000**, *156* (4), 1345–1362.
(18) Matter, M. L.; Zhang, Z. H.; Nordstedt, C.; Ruoslahti, E. *J. Cell Biol.* **1998**, *141* (4), 1019–1030.
(19) van Golen, K. L.; Bao, L. W.; Brewer, G. J.; Pienta, K. J.; Kamradt, J. M.; Livant, D. L.; Merajver, S. D. *Neoplasia* **2002**, *4* (5), 373–379.
(20) Livant, D. L. *Curr. Cancer Drug Targets* **2005**, *5* (7), 489–503.
(21) Ruoslahti, E.; Pierschbacher, M. D. *Science* **1987**, *238* (4826), 491–497.
(22) Ferris, D. M.; Moodie, G. D.; Dimond, P. M.; Gioranni, C. W. D.; Ehrlich, M. G.; Valentini, R. F. *Biomaterials* **1999**, *20* (23–24), 2323–2331.
(23) Ruoslahti, E. *Annu. Rev. Cell Dev. Biol.* **1996**, *12*, 697–715.
(24) Aota, S.; Nomizu, M.; Yamada, K. M. *J. Biol. Chem.* **1994**, *269* (40), 24756–24761.
(25) Redick, S. D.; Settles, D. L.; Briscoe, G.; Erickson, H. P. *J. Cell Biol.* **2000**, *149* (2), 521–527.
(26) Altroff, H.; Choulier, L.; Mardon, H. J. *J. Biol. Chem.* **2003**, *278* (1), 491–497.
(27) Mardilovich, A.; Craig, J. A.; McCammon, M. Q.; Garg, A.; Kokkoli, E. *Langmuir* **2006**, *22* (7), 3259–3264.
(28) Liu, J. C.; Heilshorn, S. C.; Tirrell, D. A. *Biomacromolecules* **2004**, *5* (2), 497–504.
(29) Mardilovich, A.; Kokkoli, E. *Biomacromolecules* **2004**, *5* (3), 950–957.
(30) Kokkoli, E.; Mardilovich, A.; Wedekind, A.; Rexeisen, E. L.; Garg, A.; Craig, J. A. *Soft Matter* **2006**, *2* (12), 1015–1024.
(31) Craig, J. A.; Rexeisen, E. L.; Mardilovich, A.; Shroff, K.; Kokkoli, E. *Langmuir* **2008**, *24* (18), 10282–10292.
(32) Ochsenhirt, S. E.; Kokkoli, E.; McCarthy, J. B.; Tirrell, M. *Biomaterials* **2006**, *27* (20), 3863–3874.
(33) Keselowsky, B. G.; Collard, D. M.; Garcia, A. J. *Proc. Natl. Acad. Sci. U. S. A.* **2005**, *102* (17), 5953–5957.
(34) Hynes, R. O. *Fibronectins*; Springer-Verlag: New York, 1990; p 546.
(35) Hynes, R. O. *Cell* **2002**, *110* (6), 673–687.
(36) Cukierman, E.; Pankov, R.; Stevens, D. R.; Yamada, K. M. *Science* **2001**, *294* (5547), 1708–1712.
(37) Aucoin, L.; Griffith, C. M.; Pleizier, G.; Deslandes, Y.; Sheardown, H. *J. Biomater. Sci., Polym. Ed.* **2002**, *13* (4), 447–462.
(38) Benoit, D. S. W.; Anseth, K. S. *Biomaterials* **2005**, *26* (25), 5209–5220.
(39) Kao, W. J.; Hubbell, J. A.; Anderson, J. M. *J. Mater. Sci.: Mater. Med.* **1999**, *10* (10–11), 601–605.
(40) Susuki, Y.; Hojo, K.; Okazaki, I.; Kamata, H.; Sasaki, M.; Maeda, M.; Nomizu, M.; Yamamoto, Y.; Nakagawa, S.; Mayumi, T.; Kawasaki, K. *Chem. Pharm. Bull.* **2002**, *50* (9), 1229–1232.
(41) Kim, T. I.; Jang, J. H.; Lee, Y. M.; Ryu, I. C.; Chung, C. P.; Han, S. B.; Choi, S. M.; Ku, Y. *Biotechnol. Lett.* **2002**, *24* (24), 2029–2033.

(42) Mardilovich, A.; Kokkoli, E. *Langmuir* **2005**, *21* (16), 7468–7475.
(43) Demirgoz, D.; Garg, A.; Kokkoli, E. *Langmuir* **2008**, *24* (23), 13518–13524.
(44) Garg, A.; Tisdale, A. W.; Haidari, E.; Kokkoli, E. *Int. J. Pharm.* **2009**, *366* (1–2), 201–210.
(45) Demirgoz, D.; Pangburn, T. O.; Davis, K. P.; Lee, S.; Bates, F. S.; Kokkoli, E. *Soft Matter* **2009**, *5* (10), 2011–2019.
(46) Atchison, N. A.; Fan, W.; Papas, K. K.; Hering, B. J.; Tsapatsis, M.; Kokkoli, E. *Langmuir* **2010**, *26* (17), 14081–14088.
(47) Shroff, K.; Rexeisen, E. L.; Arunagirinathan, M. A.; Kokkoli, E. *Soft Matter* **2010**, *6* (20), 5064–5072.
(48) Garg, A.; Kokkoli, E. *Curr. Pharm. Biotechnol.* **2011**, *12* (8), 1135–1143.
(49) Rexeisen, E. L.; Fan, W.; Pangburn, T. O.; Taribagil, R. R.; Bates, F. S.; Lodge, T. P.; Tsapatsis, M.; Kokkoli, E. *Langmuir* **2010**, *26* (3), 1953–1959.
(50) Pangburn, T. O.; Bates, F. S.; Kokkoli, E. Submitted 2011.
(51) Aplin, A. E.; Howe, A. K.; Juliano, R. L. *Curr. Opin. Cell Biol.* **1999**, *11* (6), 737–744.
(52) Schwartz, M. A. *Cancer Res.* **1993**, *53* (7), 1503–1506.
(53) Hanks, S. K.; Calalb, M. B.; Harper, M. C.; Patel, S. K. *Proc. Natl. Acad. Sci. U. S. A.* **1992**, *89* (18), 8487–8491.
(54) Hanks, S. K.; Polte, T. R. *Bioessays* **1997**, *19* (2), 137–145.
(55) Howe, A.; Aplin, A. E.; Alahari, S. K.; Juliano, R. L. *Curr. Opin. Cell Biol.* **1998**, *10* (2), 220–231.
(56) Parsons, J. T.; Martin, K. H.; Slack, J. K.; Taylor, J. M.; Weed, S. A. *Oncogene* **2000**, *19* (49), 5606–5613.
(57) Cary, L. A.; Guan, J.-L. *Front. Biosci.* **1999**, *4* (Jan 15), D102–113.
(58) Calalb, M. B.; Polte, T. R.; Hanks, S. K. *Mol. Cell. Biol.* **1995**, *15* (2), 954–963.
(59) Hamadi, A.; Bouali, M.; Dontenwill, M.; Stoeckel, H.; Takeda, K.; Ronde, P. *J. Cell Sci.* **2005**, *118* (19), 4415–4425.
(60) Ruest, P. J.; Roy, S.; Shi, E. G.; Mernaugh, R. L.; Hanks, S. K. *Cell Growth Differ.* **2000**, *11* (1), 41–48.
(61) Legate, K. R.; Wickstrom, S. A.; Fassler, R. *Genes Dev.* **2009**, *23* (4), 397–418.
(62) Danen, E. H. J.; Yamada, K. M. *J. Cell. Physiol.* **2001**, *189* (1), 1–13.
(63) Schwartz, M. A.; Assoian, R. K. *J. Cell Sci.* **2001**, *114* (14), 2553–2560.
(64) Danen, E. H. J.; Sonnenberg, A. *J. Pathol.* **2003**, *200* (4), 471–480.
(65) Walker, J. L.; Assoian, R. K. *Cancer Metastasis Rev.* **2005**, *24* (3), 383–393.
(66) Mettouchi, A.; Klein, S.; Guo, W. J.; Lopez-Lago, M.; Lemichez, E.; Westwick, J. K.; Giancotti, F. G. *Mol. Cell* **2001**, *8* (1), 115–127.
(67) Chen, H. C.; Appeddu, P. A.; Isoda, H.; Guan, J. L. *J. Biol. Chem.* **1996**, *271* (42), 26329–26334.
(68) Webb, D. J.; Donais, K.; Whitmore, L. A.; Thomas, S. M.; Turner, C. E.; Parsons, J. T.; Horwitz, A. F. *Nat. Cell Biol.* **2004**, *6* (2), 154–161.
(69) Walker, J. L.; Fournier, A. K.; Assoian, R. K. *Cytokine Growth Factor Rev.* **2005**, *16* (4–5), 395–405.
(70) Schlaepfer, D. D.; Broome, M. A.; Hunter, T. *Mol. Cell. Biol.* **1997**, *17* (3), 1702–1713.
(71) Schlaepfer, D. D.; Hunter, T. *J. Biol. Chem.* **1997**, *272* (20), 13189–13195.
(72) Zhao, J. H.; Reiske, H.; Guan, J. L. *J. Cell Biol.* **1998**, *143* (7), 1997–2008.
(73) Zhao, J.; Pestell, R.; Guan, J. L. *Mol. Biol. Cell* **2001**, *12* (12), 4066–4077.
(74) Cox, B. D.; Natarajan, M.; Stettner, M. R.; Gladson, C. L. *J. Cell Biochem.* **2006**, *99* (1), 35–52.
(75) Quelle, D. E.; Ashmun, R. A.; Shurtleff, S. A.; Kato, J. Y.; Barsagi, D.; Roussel, M. F.; Sherr, C. J. *Genes Dev.* **1993**, *7* (8), 1559–1571.
(76) Resnitzky, D.; Gossen, M.; Bujard, H.; Reed, S. I. *Mol. Cell. Biol.* **1994**, *14* (3), 1669–1679.
(77) Huang, S.; Chen, C. S.; Ingber, D. E. *Mol. Biol. Cell* **1998**, *9* (11), 3179–3193.
(78) Berndt, P.; Fields, G. B.; Tirrell, M. *J. Am. Chem. Soc.* **1995**, *117* (37), 9515–9522.
(79) Hautanen, A.; Gailit, J.; Mann, D. M.; Ruoslahti, E. *J. Biol. Chem.* **1989**, *264* (3), 1437–1442.
(80) Takagi, J.; Strokovich, K.; Springer, T. A.; Walz, T. *EMBO J.* **2003**, *22* (18), 4607–4615.
(81) Kemmer, G.; Keller, S. *Nature Protocols* **2010**, *5* (2), 267–281.
(82) Shaffer, J. F.; Kensler, R. W.; Harris, S. P. *J. Biol. Chem.* **2009**, *284* (18), 12318–12327.
(83) Hansma, H. G.; Clegg, D. O.; Kokkoli, E.; Oroudjev, E.; Tirrell, M. *Methods Cell-Matrix Adhes.* **2002**, *69*, 163–193.
(84) Petrie, T. A.; Capadona, J. R.; Reyes, C. D.; Garcia, A. J. *Biomaterials* **2006**, *27* (31), 5459–5470.
(85) Shi, Q.; Boettiger, D. *Mol. Biol. Cell* **2003**, *14* (10), 4306–4315.
(86) Kim, S. H.; Kim, J. H.; Akaike, T. *FEBS Lett.* **2003**, *553* (3), 433–439.
(87) Thibault, G. *Mol. Pharmacol.* **2000**, *58* (5), 1137–1145.
(88) Garcia, A. J.; Vega, M. D.; Boettiger, D. *Mol. Biol. Cell* **1999**, *10* (3), 785–798.
(89) Richman, G. P.; Tirrell, D. A.; Asthagiri, A. R. *J. Controlled Release* **2005**, *101* (1–3), 3–12.
(90) Miller, T.; Boettiger, D. *Langmuir* **2003**, *19* (5), 1723–1729.
(91) Litvinov, R. I.; Shuman, H.; Bennett, J. S.; Weisel, J. W. *Proc. Natl. Acad. Sci. U. S. A.* **2002**, *99* (11), 7426–7431.
(92) Krammer, A.; Lu, H.; Isralewitz, B.; Schulten, K.; Vogel, V. *Biophys. J.* **1999**, *76* (1), A9–A9.
(93) Asthagiri, A. R.; Nelson, C. M.; Horwitz, A. F.; Lauffenburger, D. A. *J. Biol. Chem.* **1999**, *274* (38), 27119–27127.